# Complement-Like Protein TEP1 Is a Determinant of Vectorial Capacity in the Malaria Vector *Anopheles gambiae*

Stephanie Blandin,[1] Shin-Hong Shiao,[2]
Luis F. Moita,[1,4] Chris J. Janse,[3] Andrew P. Waters,[3]
Fotis C. Kafatos,[1] and Elena A. Levashina[1,2,*]
[1]European Molecular Biology Laboratory
Meyerhofstrasse 1
69117 Heidelberg
Germany
[2]UPR 9022 du CNRS
Institut de Biologie Moléculaire et Cellulaire
15 rue René Descartes
67084 Strasbourg Cedex
France
[3]Department of Parasitology
Leiden University Medical Centre
Postbus 9600 RC
Leiden
The Netherlands

## Summary

*Anopheles* mosquitoes are major vectors of human malaria in Africa. Large variation exists in the ability of mosquitoes to serve as vectors and to transmit malaria parasites, but the molecular mechanisms that determine vectorial capacity remain poorly understood. We report that the hemocyte-specific complement-like protein TEP1 from the mosquito *Anopheles gambiae* binds to and mediates killing of midgut stages of the rodent malaria parasite *Plasmodium berghei*. The dsRNA knockdown of *TEP1* in adults completely abolishes melanotic refractoriness in a genetically selected refractory strain. Moreover, in susceptible mosquitoes this knockdown increases the number of developing parasites. Our results suggest that the TEP1-dependent parasite killing is followed by a TEP1-independent clearance of dead parasites by lysis and/or melanization. Further elucidation of the molecular mechanisms of TEP1-mediated parasite killing will be of great importance for our understanding of the principles of vectorial capacity in insects.

## Introduction

Human malaria is one of the most devastating diseases, especially in Sub-Saharan Africa. Every year, 300 to 500 million people suffer from this disease and more than one million die, mostly children under the age of 5 (Snow et al., 1999). The causative agents of malaria are protozoan parasites of the genus *Plasmodium*, which are transmitted to an *Anopheles* mosquito vector when the female mosquito takes an infected bloodmeal. To become infective to the next host, the parasite must undergo a complex developmental cycle in the mosquito.

*Correspondence: e.levashina@ibmc.u-strasbg.fr
[4]Present address: Center for Immunology and Inflammatory Diseases, Massachusetts General Hospital, 149 13th Street, Charlestown, Massachusetts 02129.

Within the insect midgut, *Plasmodium* gametocytes are rapidly activated to produce gametes. Fertilization leads to the formation of zygotes which, 16–20 hr later, transform into motile ookinetes. Approximately 24 hr after an infectious bloodmeal, the ookinetes invade and cross the midgut epithelium, reaching the basal side of the midgut where they form protected capsules called oocysts. In the next 10 days, within each oocyst, a meiotic cycle and several ongoing rounds of mitosis produce thousands of haploid sporozoites. After maturation (14–16 days after the infectious bloodmeal), sporozoites are released into the mosquito hemocoel and migrate to the salivary glands which they invade. The parasite cycle in the mosquito is completed when this vector injects infective sporozoites into a new vertebrate host during a subsequent blood feeding.

Most mosquito species are not permissive for *Plasmodium* parasites and only a limited number of dedicated *Plasmodium–Anopheles* combinations cause malaria in a particular group of vertebrates. Thus, mosquito-parasite interactions constitute a critical aspect of disease transmission and are a potential target for efforts to control malaria. *A. gambiae* is the most important vector of human malaria in much of Africa. We have chosen as a laboratory model the infection of *A. gambiae* by *P. berghei*, a rodent malaria parasite, to study mosquito-parasite interactions and thus comprehend the biological principles of mosquito antiparasitic responses in a simple and safe system.

It has long been known that within the same species, mosquitoes display genetic variation in their susceptibility to parasites. Strains refractory to various malarias have been selected and studied, mostly morphologically (reviewed in Vargas, 1949). In the present study, we made use of a refractory strain of *A. gambiae* (R), which completely aborts development of a number of malaria parasites, including the simian parasite *P. cynomolgi* B. Refractoriness is manifested by melanotic encapsulation of the ookinete, after it completes its passage through the mosquito midgut (Collins et al., 1986). The genetic control of refractoriness appears to be complex. It not only involves several quantitative trait loci, but also the relative contribution of each locus to oocyst encapsulation varies with the species of parasites (Zheng et al., 1997, 2003). A different refractory mechanism resulting in complete lysis of *P. gallinaceum* ookinetes in the midgut was reported in *A. gambiae* (Vernick et al., 1995). To date, the molecular mechanisms underlying both types of refractoriness, and more generally parasite recognition and killing, are not well understood.

We are interested in the mechanisms of parasite recognition and have chosen a family of *t*hioester-containing *p*roteins (TEPs) as potential candidate recognition molecules. In vertebrates, members of this family comprise the universal protease inhibitors $\alpha_2$-macroglobulins, and the complement factors C3/C4/C5, which are involved in labeling pathogens and triggering their disposal through phagocytosis or cell lysis. A family of 19 TEPs has been identified in the genome of *A. gambiae* (Christophides et al., 2002) and one of these, *TEP1*, has

been studied in detail (Levashina et al., 2001). TEP1 is an acute phase glycoprotein secreted by mosquito hemocytes into the hemolymph. Similarly to its vertebrate complement homologs, it is cleaved shortly after septic injury. Moreover, the cleaved C-terminal part of the protein binds to the surfaces of gram-positive and gram-negative bacteria through the conserved thioester bond and labels gram-negative bacteria for clearance by phagocytosis in vitro.

The properties of TEP1 to recognize microorganisms and target them for destruction led us to investigate the possibility, and obtain molecular evidence, that TEP1 is one of the mosquito factors that determine vectorial capacity in *A. gambiae*. In this study, we make use of a GFP-expressing strain of *P. berghei* and demonstrate that parasite killing in both susceptible and refractory mosquitoes is mediated by direct binding of the TEP1 protein to the surface of ookinetes. The essential role of TEP1 in parasite killing is further supported by double-stranded RNA (dsRNA) knockdown experiments: in susceptible mosquitoes, the knockdown of *TEP1* results in a 5-fold increase in the number of oocysts developing on the midgut, and in the refractory strain the knockdown completely abolishes parasite melanization, thus converting refractory mosquitoes into susceptible. We propose a model for TEP1 function, stressing the differences between susceptible and refractory mosquitoes regarding the kinetics of TEP1 binding, parasite killing, and clearance. Furthermore, we show that *TEP1* is encoded by two distinct alleles, *TEP1s* and *TEP1r* that appear to be specific to the susceptible and the melanotically encapsulating refractory strain, respectively. These results document the important role of mosquito immune responses, especially those orchestrated by hemocytes, in the establishment of vectorial capacity and transmission of malaria. Further elucidation of the molecular mechanisms of TEP1 killing will provide important insights toward development of antimalarial strategies.

## Results

### Binding of TEP1 to *P. berghei*

In vertebrates, complement factors bind covalently to target surfaces, opsonizing them for phagocytosis or initiating the formation of a lytic membrane attack complex (for review, see Carroll and Fischer, 1997; Law and Dodds, 1997). TEP1 binds to the surface of both gram+ and gram− bacteria in a thioester-dependent manner and promotes phagocytosis of bacteria in vitro and in vivo (Levashina et al., 2001; L.F.M., S.B., F.C.K., and E.A.L., unpublished data). To investigate whether TEP1 also recognizes *Plasmodium* parasites, we first performed immunohistochemical analysis of susceptible (S) mosquito midgut tissues infected with *P. berghei*, using rabbit polyclonal antibodies directed against the C-terminal fragment of TEP1 (Levashina et al., 2001). *A. gambiae* females of the S strain were infected with *P. berghei*, dissected at selected time points and analyzed by confocal microscopy. No TEP1-positive signal was observed in the midgut epithelial cells at any time. Instead, specific expression of *TEP1* was detected in the mosquito hemocytes attached to the midgut and Mal-
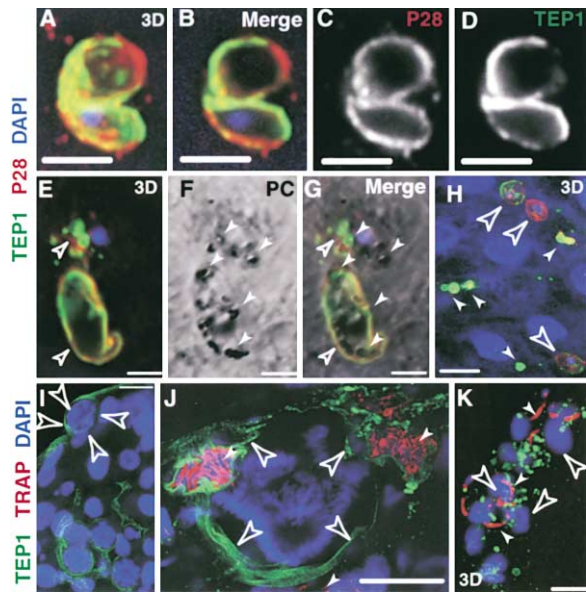


Figure 1. Binding of TEP1 to *P. berghei* Parasites in Susceptible Mosquitoes

Confocal sections (B-D, I–J) and 3D reconstructions (A, E–H, and K) of midgut tissues from susceptible mosquitoes at different time points after infection. Triple staining showing TEP1 in green, a parasite surface protein in red (P28 in A–H or TRAP in J and K) and nucleic acids in blue.

(A–D) TEP1 was detected on the surface of ookinetes 22 hpi. The colocalization of P28 (C, red channel) and TEP1 (D, green channel) is evidenced in the merged image (B).

(E–G) TEP1-labeled ookinetes display a lytic phenotype 24 hpi. Bubbles are of parasite origin as evidenced by the presence of P28 (E, open arrowheads) and hemozoine granules (F, phase contrast image, filled arrowheads) in the merged image (G).

(H) Two days pi, ookinetes (filled arrowheads) are heavily labeled with TEP1, whereas young oocysts (open arrowheads) display weak or no opsonization.

(I–K) Later in development, oocysts are covered by TEP1 (open arrowheads in I and J at 11 and 16 dpi, respectively). Note that sporozoites (filled arrowheads in J and K) are already visible in matured oocysts (J). No TEP1 is detected on sporozoites (K). Rare evidence of contact between mosquito hemocytes (open arrowheads) and sporozoites (K). Scale bars in μm: (A–G), 2; (H–J), 10; (K), 5.

pighian tubules. TEP1 staining in hemocytes was more pronounced at 24 and 48 hr postinfection (hpi) as compared to uninfected controls (Levashina et al., 2001 and data not shown). Importantly, starting at 24 hpi, TEP1 appeared on the surface of some ookinetes (Figures 1A–1G), as evidenced by colocalization of the signals for TEP1 and for the ookinete surface protein P28 (Simonetti et al., 1993). The number of ookinetes positive for TEP1 increased with time and attained a maximum at approximately 48 hpi (data not shown), when the surviving parasites have completed their migration through the midgut epithelium and rest in the extracellular space, between the membrane folds of the basal labyrinth of the midgut cells, facing the basal lamina. We have never observed TEP1 labeling of all ookinetes in the susceptible strain. Between 22 and 48 hpi, parasites smaller than normal and strongly labeled with TEP1 were often detected. These parasites were usually associated with P28-positive blobs and lacked nuclear staining (Figures

1E–1H). This morphology suggested that these parasites might have been killed during the invasion process.

We have also examined whether TEP1 binds to later stages of parasites. Shortly after reaching the basal lamina, ookinetes round up and transform into young oocysts. At 48 hpi, nondeveloping and presumably dead, ookinetes were heavily labeled with TEP1, whereas developing oocysts showed only weak and patchy TEP1 labeling (Figure 1H, filled and outlined arrowheads, respectively). However, at 11 days postinfection (dpi) well-developed oocysts were covered by abundant TEP1-positive material, and the morphology suggested that TEP1 was associated with components of the basal lamina in which the oocysts are embedded (Figures 1I and 1J). In contrast, sporozoites that develop from oocysts and are stained with specific antibodies against the *thrombospondin-related anonymous protein* (TRAP) never displayed TEP1 staining on the surface, indicating that TEP1 does not directly interact with this haploid form of the parasite (Figures 1J and 1K). Even in exceptional cases when clusters of mosquito hemocytes were in contact with sporozoites, no colocalization was detected between the TEP1 and TRAP signals (Figure 1K).

We next examined TEP1 binding to *P. berghei* in the refractory (R) strain. As in S mosquitoes, TEP1 was found to bind to ookinetes in a time-dependent manner, but clearly with faster kinetics: most of the parasites were labeled with TEP1 as early as 24 hpi (Figures 2C and 3E). The binding of TEP1 to ookinetes was further confirmed by electron microscopy (Figures 2A and 2B). It often correlated with perturbations in the P28 signal on ookinete surface, parasite blebbing, condensation and degeneration of nuclei and, in extreme cases, localization of P28 inside the degenerated parasites (Figures 2D–2G). At later time points, all detectable parasites in the R mosquitoes were melanized and, therefore, opaque. The early and extensive TEP1 binding to ookinetes in the basal labyrinth correlates with ookinete melanization, which begins at the same time and location (24–36 hpi). We explored the potential role of TEP1 in melanization in more detail by confocal microscopy using specific antibodies against TEP1 and against the conserved copper binding domain of PPO6 (Müller et al., 1999). A PPO-positive signal was detected in the cytoplasm of hemocytes but not in the midgut cells, indicating that PPOs, like TEP1, are produced by the mosquito blood cells and are released into the hemolymph (data not shown). The hemocytes often coexpress PPOs and TEP1 (data not shown). Importantly, the PPO signal was detected only on the surface of TEP1-labeled ookinetes and yet, no precise colocalization between TEP1 and PPOs was observed (Figures 2F–2I). This suggests that TEP1 is associated with ookinete melanization but is not directly involved in the tethering of the PPO complex on the parasite surface. The PPO-positive layer was later surrounded by a second layer of TEP1, reminiscent of the TEP1 deposition on oocysts described for S mosquitoes (compare Figures 2H and 1I).

## Parasite Losses during Midgut Invasion

Our results indicate that TEP1 is able to recognize and bind to specific developmental stages of *P. berghei*. Potentially, this binding might serve two opposing func-
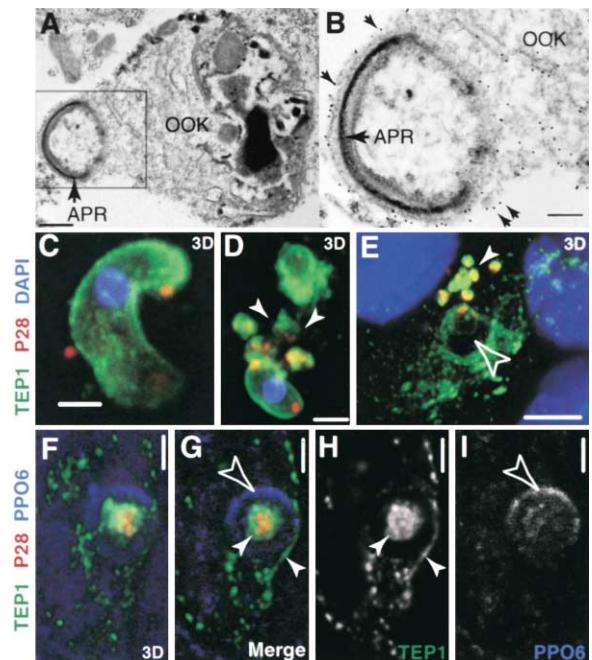


Figure 2. Binding of TEP1 to *P. berghei* Parasites in Refractory Mosquitoes

(A) The electron micrograph (30 hpi) shows the apical part of an ookinete (OOK), and its intracellular apical polar ring (APR).

(B) A close up view of the boxed area in (A). Binding of TEP1 to ookinetes is evidenced by gold particles on the parasite surface (arrows).

(C–F) 3D reconstructions and (G–I) confocal sections of midgut tissues at different time points after infection. Triple staining as in Figure 1 with P28 in red. Ookinetes labeled with TEP1 (C, 24 hpi) display a lytic phenotype as in S mosquitoes (compare small arrowheads in D, E, 32 hpi, and Figure 1E). Melanized ookinetes are covered with a second layer of TEP1 (E, big arrowhead, and data not shown).

(F–I) The parasite is surrounded by concentric layers of TEP1, PPO, and TEP1 (44 hpi). Note the absence of colocalization between TEP1 (H, green channel, small arrowhead) and PPOs (I, blue channel, open arrowhead) in the merged image (G). Scale bars in μm: (A), 0.5; (B), 0.2; (C, D, F–I), 2; (E), 5.

tions: (1) help parasite invasion or, (2) limit parasite development. To distinguish between these two hypotheses, we monitored quantitatively the development of *P. berghei* and the kinetics of TEP1 binding in both S and R mosquitoes, using a transgenic parasite strain PbGFP$_{CON}$ that expresses GFP under control of the *elF1* gene promoter throughout its life cycle in the mosquito (Alavi et al., 2003). Female mosquitoes were blood-fed on PbGFP$_{CON}$ infected mice and dissected 24 and 32 hr later for analysis by multichannel confocal microscopy. In these experiments, in addition to GFP fluorescence, we used P28 antibodies to detect parasites and TEP1 antibodies to follow their opsonization.

Surprisingly, the only universal (although occasionally weak) marker for the parasites was P28 staining (Figures 3A and 3C). Only a minority of ookinetes expressed GFP at 24 hpi, both in S and especially in R mosquitoes (Figure 3E, 38% and 14%, respectively). The number of GFP-positive ookinetes decreased with time and, at 32 hpi, it was down to 20% and 3% in S and R mosquitoes,
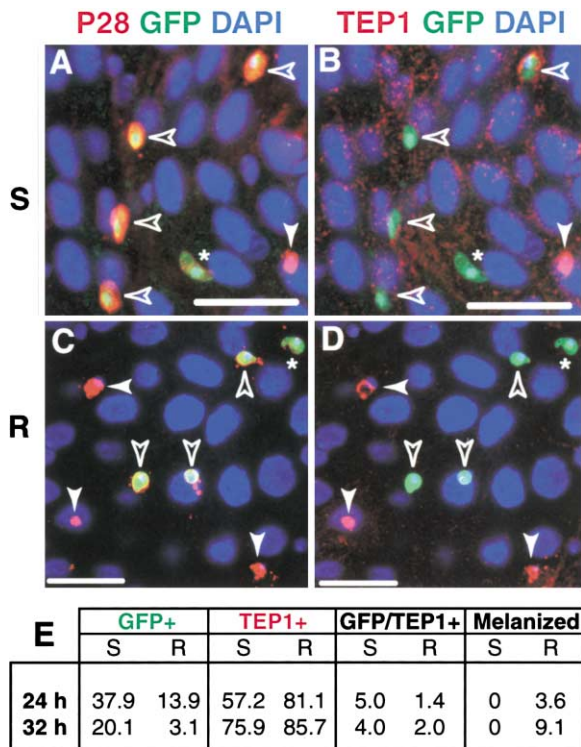
## P28 GFP DAPI    TEP1 GFP DAPI



**Figure 3. Parasite Killing in the Mosquito Midgut**

Double staining of midgut tissues of susceptible (A–B) and refractory (C–D) mosquitoes 24 hpi with the GFP-parasite: (A, C): P28 in red; GFP in green; (B, D): TEP1 in red; GFP in green. Nucleic acids are in blue. Scale bars are equal to 20 μm. Parasites showing a strong P28 staining and GFP fluorescence are indicated with open arrowheads. Filled arrowheads point to GFP-negative parasites. Parasites displaying a weak P28 staining are indicated with asterisks. Most of the TEP1-labeled ookinetes have lost their GFP staining (B and D, filled arrowheads). Table (E) shows percentages of ookinetes positive for GFP (GFP+), for TEP1 (TEP1+), for both (GFP/TEP1+) or melanized, in S and R mosquitoes at 24 and 32 hpi. The results of three independent experiments were highly consistent (1000–3000 ookinetes were counted for each time point and mosquito strain) and one representative experiment is shown.

| E | GFP+ | | TEP1+ | | GFP/TEP1+ | | Melanized | |
|---|---|---|---|---|---|---|---|---|
| | S | R | S | R | S | R | S | R |
| **24 h** | 37.9 | 13.9 | 57.2 | 81.1 | 5.0 | 1.4 | 0 | 3.6 |
| **32 h** | 20.1 | 3.1 | 75.9 | 85.7 | 4.0 | 2.0 | 0 | 9.1 |

respectively. Conversely, TEP1-decorated parasites were always a majority, their numbers increased over time, and they were always more numerous in R than in S mosquitoes: at 24 hpi 81% versus 57%, respectively, and at 32 hpi 86% versus 76% (Figure 3E). Notable observations were that GFP-negative ookinetes were heavily labeled with TEP1 (Figures 3B and 3D, filled arrowheads), and that many of them had also lost nuclear staining, suggesting that the lack of GFP fluorescence reflects parasite death. Only very rarely did TEP1-positive ookinetes show GFP fluorescence (Figure 3E, no higher than 5%); possibly, these double positives represent an early stage in a process that begins with TEP1 binding and proceeds with loss of GFP fluorescence, nuclear disintegration, and parasite elimination. The key observation was that binding of TEP1, loss of parasite fluorescence, and parasite death proceeded in parallel, faster in R than in S mosquitoes. All but about 5% of the parasites were killed by 32 hpi in the refractory strain (as indicated by lack of GFP fluorescence or mela-

nization), whereas in the susceptible strain approximately 24% of the parasites survived.

**TEP1 Limits Parasite Development**

If TEP1 binding is essential for parasite killing, its absence should result in higher oocyst numbers in the mosquito midguts. The in vivo expression of *TEP1* was silenced by injecting dsRNA corresponding to *TEP1* into the thorax of young susceptible females; controls received dsRNA of unrelated genes. The efficacy of the knockdown (KD) was confirmed by immunoblotting: the 165 kDa full-length and 80 kDa cleaved forms of TEP1 (Levashina et al., 2001) were detected in hemolymph samples of control but not *dsTEP1*-treated mosquitoes (Figure 4A). Four days after dsRNA injection, mosquitoes were fed on GFP-parasite infected mice, and 24 hr later immunohistochemistry further confirmed the efficacy of the KD, as no TEP1 labeling of parasites was detected in *dsTEP1*-treated mosquitoes (compare Figures 4B and 4C). The absence of TEP1 was correlated with substantially higher levels of ookinete survival evidenced by GFP expression (see below). Careful analysis detected a number of parasites that were negative for GFP as well as TEP1, suggesting that more than one mechanism controls parasite loads in *A. gambiae* (Figure 4C, arrowheads).

In control experiments, mosquitoes were injected with either *dsGFP* or *dsLacZ* RNAs; the respective mean numbers of fluorescent oocysts were indistinguishable (data not shown), indicating that the expression of a parasite-borne gene (*GFP* in this case) cannot be silenced when dsRNA is delivered to mosquitoes. In three independent experiments performed on susceptible mosquitoes, we observed a 5-fold increase in the mean number of oocysts in *dsTEP1* mosquitoes as compared to *dsLacZ* controls, as well as a uniquely large class of superinfected mosquitoes with >300 oocysts per midgut (Figures 4D, 4E, and 4P). These results clearly demonstrate that *A. gambiae* senses the malaria parasites and actively limits their development in a TEP1-dependent manner, even in the susceptible strain. The parasites that remained GFP-labeled successfully developed into oocysts and produced infectious sporozoites that efficiently invaded the mosquito salivary glands (Figures 4F and 4G).

We have also silenced *TEP1* expression in R mosquitoes by injecting L3-5 females with *dsTEP1*, and with *dsGFP* or *dsLacZ* as controls. The efficacy of the knockdown was again confirmed by immunoblotting (Figure 4A) and by immunohistochemical analysis (Figures 4H and 4I), which demonstrated that *dsTEP1* completely depleted TEP1 from the hemolymph, resulting in the absence of parasite opsonization. Melanized ookinetes and young oocysts were detected only in the midguts of control mosquitoes starting from 24 hpi and persisting throughout the lifetime, demonstrating that after melanization parasites remain in the midgut tissues until the end of mosquito life (Figures 4J, 4K, and data not shown). Strikingly, we did not find any single melanized parasite in *dsTEP1*-treated R mosquitoes; instead, green fluorescent oocysts developed normally and released sporozoites (Figures 4L–4N). As all parasites are melanized in control R mosquitoes, we compared the number of sur-
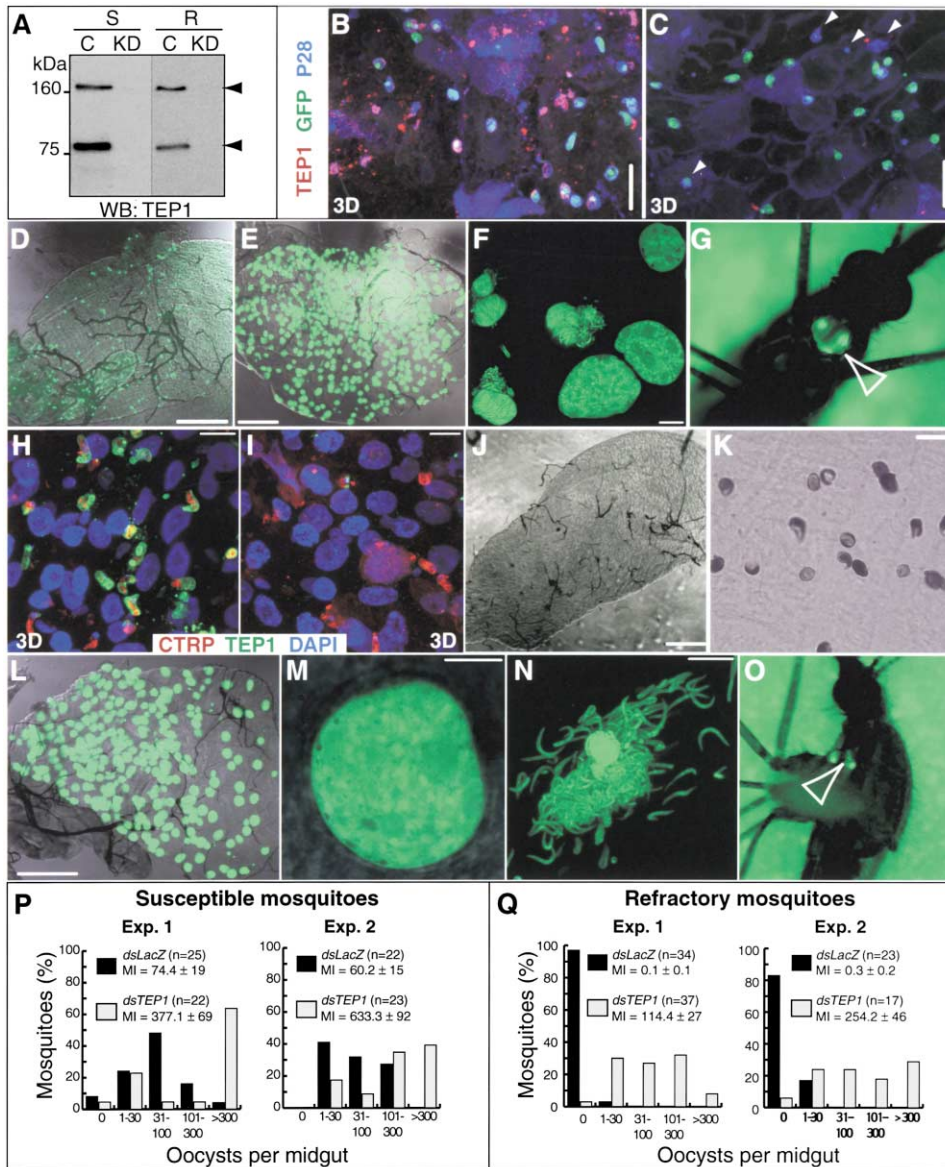
**Figure 4. Role of TEP1 in the Mosquito Antiparasitic Response**

(A) dsRNA knockdown of *TEP1* in adult susceptible (S) and refractory (R) females. The full-length and processed forms of TEP1 (arrowheads) were detected by immunoblotting using 7% SDS PAGE in the hemolymph of control mosquitoes treated with *dsGFP* (S and R, C) but not in the hemolymph of *dsTEP1*-treated mosquitoes (S and R, KD).

(B–O) Fluorescence microscopy of midguts and salivary glands of susceptible (B–G) and refractory (H–O) mosquitoes infected with the GFP-parasite. Phase contrast and GFP fluorescence are merged in (D–E) and (J–M), only the GFP fluorescence is displayed in (F–G) and (N–O).

(B–C) Double staining of midgut tissues of S mosquitoes treated with *dsLacZ* (B) and *dsTEP1* (C) 32 hpi showing the absence of TEP1 in *dsTEP1* mosquitoes: TEP1 in red; GFP in green; P28 in blue. Note the presence of parasites that do not express GFP in *dsTEP1* mosquitoes (C, arrowheads).

(D–G) Development of GFP-parasites in *dsLacZ* (D) and *dsTEP1* (E–G) mosquitoes. Note higher infection rates in *dsTEP1* midguts 11 dpi (E). In *dsTEP1* mosquitoes, oocysts develop normally (F, 11 dpi) and produce infective sporozoites that invade salivary glands (arrowhead in G, 21 dpi).

(H–I) Triple staining of midgut tissues of R mosquitoes 24 hpi (CTRP in red; TEP1 in green; nucleic acids in blue) demonstrating the absence of TEP1 in *dsTEP1*-treated mosquitoes.

(J–K) Ookinetes melanization in refractory mosquitoes 48 hpi.

(L–O) The knockdown of *TEP1* in R mosquitoes completely abolishes the melanization phenotype. Ookinetes successfully transform into oocysts (L, M, 10 dpi) and further mature into sporozoites (N, 10 dpi) that invade salivary glands (arrowhead in O, 21 dpi).

(P–Q) Frequency distribution of oocysts in mosquito midguts after dsRNA knockdown in susceptible (P) and refractory (Q) mosquitoes. Control (*dsLacZ*) and *dsTEP1*-treated (*dsTEP1*) mosquitoes were infected with the GFP-parasite, dissected 10 days later, and the number of oocysts on each midgut was counted. Results of two out of four independent experiments for each mosquito strain are shown. n, number of mosquitoes per experiment, MI, mean intensity of infection plus/minus standard error.

Scale bars in $\mu$m: (D, E, J, L), 200; (B, C, F, M, N), 20; (H, I, K), 10.
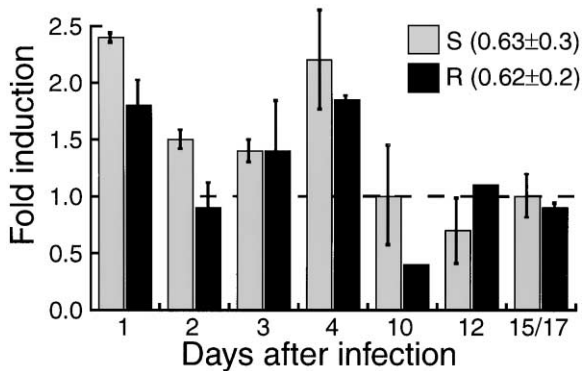
Figure 5. Inducibility of *TEP1* Expression upon *P. berghei* Infection

Quantitative real-time PCR using specific primers and probes for *TEP1s* in susceptible (S) and *TEP1r* in refractory (R) mosquitoes. The levels of *TEP1* transcript at various time points after infection were normalized to the internal control transcript for ribosomal protein S7. Results are shown as fold induction relative to the 6 hpi control. Absolute values for this time point are shown in brackets in the upper right. For most of the time points, experiments were performed 3 to 4 times (error bars indicate standard errors). Results for 10 and 12 dpi in R mosquitoes are from one experiment.

viving parasites in *dsTEP1* R mosquitoes to that of control S mosquitoes. In three independent experiments, the number of developing parasites in R mosquitoes after *dsTEP1* treatment was 2- to 3-fold higher than in *dsLacZ* S mosquitoes. However, in contrast to the results of *dsTEP1* knockdown in S mosquitoes, it never reached the 5-fold increase and superinfected mosquitoes with >300 oocysts per midgut did not represent a major class in *dsTEP1* R mosquitoes (Figures 4P and 4Q), indicating that the melanotic refractoriness is a complex phenomenon which requires coordinated action of a number of genes, including *TEP1*. Mature sporozoites successfully invaded the salivary glands (Figure 4O) and were infective to a mouse (data not shown). To demonstrate that the surviving parasites did not represent a revertant clone that escaped melanization, we fed a new batch of naive (not *dsTEP1*-treated) R mosquitoes on the same mouse that had been infected with the surviving parasites. All parasites in these mosquitoes were melanized (data not shown), indicating that the normal development of parasites in the knockdown R mosquitoes was indeed due to silencing of a single gene, *TEP1*.

**Expression of *TEP1* Is Upregulated after Parasite Infection**

Distinct kinetics and efficiency of parasite killing in the S and R strains may result from a differential pattern of *TEP1* expression in these two strains. We compared the transcriptional profiles of *TEP1* by quantitative real-time PCR in whole S and R females at selected time points after infection (Figure 5). In these experiments, the expression level of *TEP1* was normalized to that of the gene encoding the ribosomal protein rpS7. At 6 hpi, no parasite-specific interactions take place and mosquitoes react mostly to the physiological changes induced by a bloodmeal (Dimopoulos et al., 2002). Therefore, the

normalized expression of *TEP1* at 6 hpi was used as a reference to determine any later induction of *TEP1*.

Transcription of *TEP1* followed an overall similar pattern in S and R mosquitoes. The relative level of TEP1 upregulation in S mosquitoes was somewhat higher than in R, judging by the absolute levels of expression at 6 hpi that were similar in these two strains ($0.63 \pm 0.3$ and $0.62 \pm 0.2$, respectively). The expression of *TEP1* was rapidly upregulated at 24 hpi, when it reached a maximum of 2.5- and 1.8-fold in the S and R strains, respectively. This was followed by a temporary depression in transcript abundance and then by a second peak of 2.2- and 1.8-fold induction at 4 dpi in S and R mosquitoes, respectively. Thus, the peak upregulation of *TEP1* expression coincided with two important steps in the development of *P. berghei* in *A. gambiae*: the passage through the columnar cells of the midgut epithelium (24 hpi) and the establishment of oocysts (beginning on day 3–4 pi, when the oocysts become surrounded by the basal lamina; Meis et al., 1989). No upregulation of *TEP1* expression was detected at the time points associated with maturation, release, and massive migration of sporozoites from the midgut oocysts to the salivary glands (Figure 5, days 10, 12, and 15/17 pi). These results suggest that *TEP1* upregulation is a mosquito response to the presence of *Plasmodium* during key early steps of infection, both in the S and R strains.

**Genomic Polymorphism of the *TEP1* Gene Correlates with Susceptible and Refractory Strains of *A. gambiae***

We have previously proposed that *TEP1* and *TEP16* are two allelic forms of the same gene and that initial annotation of *TEP16* as a distinct gene was an artifact of the automatic genome assembly (Christophides et al., 2002). To explore whether *TEP1* polymorphism could be correlated with the S and R phenotypes, *TEP1*- and *TEP16*-specific PCR primers were designed to follow the presence of the two alleles in these strains. Primers specific for *TEP1* amplified the expected fragment in S but not in R mosquitoes. Conversely, *TEP16*-specific primers produced an amplicon in R but not S mosquitoes (Figure 6D). The results of reciprocal crosses between S and R mosquitoes confirmed that these strains are homozygous for one of the two alternative alleles, *TEP1* or *TEP16*, respectively: in contrast to the homozygous parents (S and R), individual mosquitoes of the $F_1$ progeny were positive for both forms (Figure 6D). These results suggest that *TEP1* and *TEP16* are two alleles of the same gene, which by precedence will be called *TEP1*. We propose to rename the allele associated with the S strain, *TEP1s* (formerly *TEP1*) and the allele associated with the R strain, *TEP1r* (formerly *TEP16*).

The overall identity and similarity between the TEP1s and TEP1r deduced proteins are 92% and 95%, respectively. Interestingly, the differences between these two isoforms are very unevenly distributed and are mostly concentrated in one region (Figure 6A region IV, dots for single aa substitutions and triangles for clusters of at least 5 substitutions per 50 residues).

The highly polymorphic region IV (Figure 6A) corresponds to the functionally important C3d-like domain, the structure of which was previously analyzed in TEP1

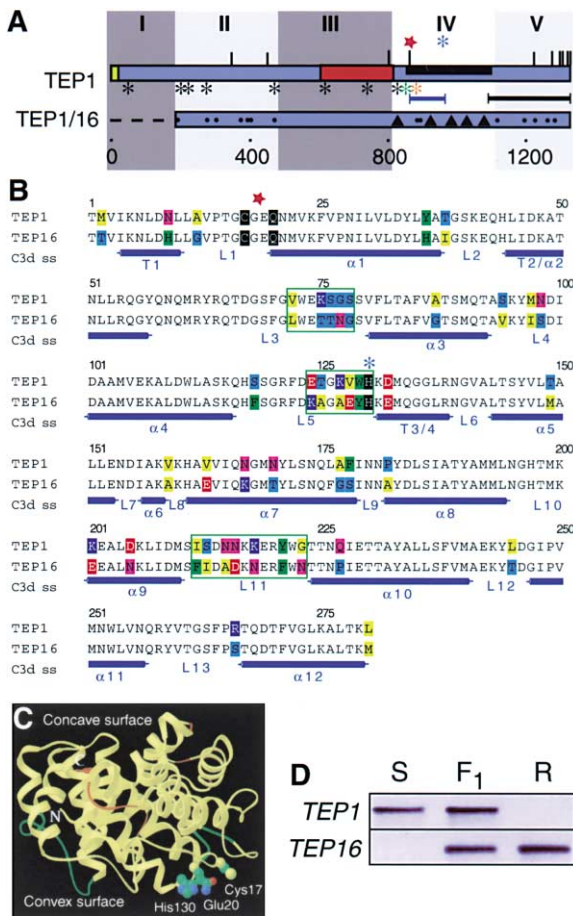Figure 6. Sequence and Structure Comparison of Two Allelic Forms of *TEP1*

(A) Schematic representation of TEP1 structure (TEP1) and sequence comparison between TEP1 and TEP16 (TEP1/16). Vertical bars indicate cysteines, the red star points to the internal thioester site and the blue asterisk to the catalytic histidine. Black, green, and orange asterisks represent conserved, TEP1-specific and TEP16-specific putative glycosylation sites, respectively. The color-filled fragments of TEP1 indicate: yellow, signal peptide; red, a region containing putative protease cleavage sites; black half-filled segment, the C3d-like region. The black horizontal bar shows the TEP1 fragment that was used to produce polyclonal antibodies and for dsRNA synthesis, the blue horizontal bar shows the fragment amplified by PCR using *TEP1* and *TEP16*-specific primers. The TEP1/TEP16 scheme shows major differences: circles for single modifications and triangles for clusters of at least 5 modifications per 50 amino acids (aa). Shaded boxes (I–V) represent regions differing in the extent of sequence conservation. The absent N-terminal sequence in TEP16 is indicated by a dashed line. Numbers correspond to aa positions in TEP1.

(B) Sequence comparison of the C3d-like region of TEP1 and TEP16. Differences between the two sequences are colored according to the aa properties. Residues of the active site are shaded in black and are indicated with a red star and blue asterisk, as in (A). Extended clusters of modifications are boxed in green. Secondary structures (turns, T, α helices, α and loops, L) are indicated below (C3d ss). Numbers correspond to aa positions in the C3d-like domain.

(C) Modeled 3D structure of the C3d-like region of TEP1 (adapted from Levashina et al., 2001). Differences between TEP1 and human C3d are indicated in brown, between TEP1 and TEP16, in green. The side chains of the active site residues are shown as ball-and-stick models.(D) PCR amplification of *TEP1* and *TEP16* in the susceptible and refractory strains. Genomic DNA from parents

by homology-based modeling (Levashina et al., 2001). The key TEP1 features are conserved in both allelic forms: (1) the canonical thioester (TE) motif (red star); (2) the catalytic histidine (blue asterisk); and (3) the cysteine residues, including a cluster of 6 cysteines at the C terminus (vertical bars). According to the model, the majority of modifications were observed in three loops (L) between putative α helices and turns (α and T blue cylinders, respectively) located on the convex side of the molecule, with loops 3 and 5 nested in close proximity to the thioester site (Figures 6B and 6C, green boxes and green loops, respectively). It is conceivable that substitutions in the thioester environment might affect the reactivity of the thioester bond leading to the different kinetics of TEP1 binding to parasites that we have detected in the S and R strains.

## Discussion

In this study, we demonstrate that the knockdown of the *TEP1* gene is sufficient to enhance substantially the number of oocysts in susceptible mosquitoes, and also to convert refractory into highly susceptible mosquitoes. We used a combination of morphological, immuno-chemical, and fluorescence markers to demonstrate that parasites suffer significant losses even in fully susceptible mosquitoes. A substantial fraction of the ookinetes is killed between 24 and 48 hpi, after they have accomplished the passage through the columnar cells of the midgut and lie in the basal labyrinth facing the basal lamina. Live ookinetes that express the *eIF1*-driven *GFP* transgene have smooth, regular edges, distinct nuclei, and generally, an even distribution of the P28 surface protein. In contrast, dead or degenerating ookinetes, identified by their complete loss of *GFP* expression, are characterized by an irregular surface, the diminution of nuclear size or even nuclear loss. They often disintegrate, as evidenced by the appearance of bubble-like projections, patchy surface, or intracellular distribution of P28. Association of ookinete death with extensive blebbing is suggestive of lytic destruction. A similar lysis phenotype of *P. gallinaceum* ookinetes was reported in *A. gambiae* by Vernick and coworkers (1995), although in this case lysis was only observed in the selected refractory strain, unlike in our experiments that identified lysis of *P. berghei* parasites in susceptible as well as refractory mosquitoes. Our observations parallel earlier morphological studies on *Culex pipiens* and *P. cathemerium* by Huff in 1934 (reviewed in Vargas, 1949), where normal and degenerate ookinetes were reported in susceptible and insusceptible mosquitoes alike. Thus, we propose that ookinete lysis in the basal labyrinth of the midgut epithelium accounts for major parasite losses associated with midgut invasion, and that it represents a general mechanism of parasite destruction even in mosquitoes that are conventionally described as susceptible.

Huff and others postulated the existence of mosquito

---

(S and R) and progeny (F1) of reciprocal crosses between susceptible G3 (S) and refractory L3-5 (R) mosquitoes was amplified using *TEP1*- and *TEP16*-specific primers.

hereditary factor(s) that determine(s) whether or not an individual mosquito will become infected after it has received an infective meal and has been kept under conditions favorable to the development of the parasite (reviewed in Vargas, 1949). Here, we identify TEP1 as one of these factors.

Several lines of evidence support the conclusion that TEP1 is a mosquito factor implicated in parasite killing and, therefore, in establishment of vector capacity in *A. gambiae*. First, TEP1 binds to the surface of ookinetes after they cross the midgut epithelium, as well as to the surface of oocysts but not of sporozoites. Second, this binding is associated with two respective peaks of transcriptional upregulation, possibly to replenish the level of circulating TEP1. Third, TEP1 binding is temporally correlated with the appearance of morphologically degenerate ookinetes. Fourth, the vast majority of TEP1-decorated ookinetes do not express the vital fluorescent marker, GFP. Some do, however, and some TEP1-positive ookinetes also have a regular shape and normal P28 surface covering. These observations suggest that TEP1 binds first and that loss of GFP fluorescence and morphological abnormalities ensue. The fifth and most stringent evidence comes from the dsRNA knockdown experiments. Indeed, *TEP1* silencing results in a 5-fold increase in parasite survival in S mosquitoes. In R mosquitoes, *TEP1* knockdown both increases parasite numbers and completely abolishes their melanization.

Taken together our results lead us to propose the following two-step model for immune responses of *A. gambiae* to *P. berghei* (Figure 7). In the first step, after crossing the midgut epithelium, parasites come in contact (within the basal labyrinth) with soluble hemolymph components, but not with hemocytes. One of the hemolymph components, TEP1, recognizes and binds to the ookinetes, causing them to die by an as yet unknown mechanism. The second step is the disposal of dead parasites by either lysis or, in the case of R mosquitoes, lysis and melanization. The model predicts that the processes of disposal of dead parasites (e.g., melanotic encapsulation and lysis) are controlled by genes other than *TEP1*. It is notable that TEP1 binding to and killing of parasites occurs in both R and S mosquitoes, albeit more slowly in the latter. It is tempting to speculate that TEP1 may function as a complement-like factor, with the covalent binding of its C-terminal part recruiting the formation of a structure similar to the membrane attack complex in mammals, and directing killing of the parasite. Detection of a small number of dead ookinetes that are not labeled with TEP1 in the knockdown experiments suggests that *TEP1* is not the only mosquito gene that controls parasite development and that other genes and gene cascades act in concert to keep the parasite load low during infection.

We stress two major differences between S and R strains. The first is related to the kinetics and efficiency of ookinete killing: approximately 80% of the ookinetes are killed in S mosquitoes by 32 hpi, whereas 100% of the parasites are killed by the same time in the R strain, 80% of which are dead already at 24 hpi. The second difference pertains to the disposal of dead parasites: lysis in S mosquitoes and lysis and melanization in the encapsulating refractory strain.

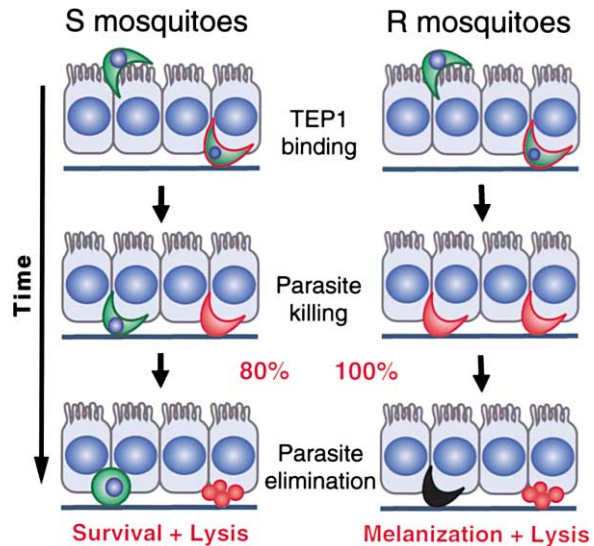So far we did not address the role of the thioester in



Figure 7. Model for the Role of TEP1 in the Antiparasitic Response of Susceptible (S) and Refractory (R) Mosquitoes

Banana-shaped ookinetes (green) traverse the mosquito midgut epithelium (represented as a cell layer, with microvilli on the lumen side) to reach the basal lamina (thick line) where they become labeled with TEP1 (red line around ookinetes). This labeling targets parasites for killing. Dead parasites (red) loose their nucleus (blue), and are eliminated. Two major differences are observed between susceptible and refractory mosquitoes. First, all parasites are killed in R mosquitoes whereas in S mosquitoes, 20% of parasites survive and transform into oocysts (round and green). Second, in S mosquitoes, dead parasites are disposed by lysis (red balls), whereas in R mosquitoes both lysis and melanization (black) are observed.

parasite binding. Further mutant analysis of the efficiency of TEP1 binding to the parasites will provide important information for structure-function analysis of this and other thioester-containing proteins. We have earlier reported proteolytic cleavage of TEP1 in the hemolymph of wounded or bacteria-infected mosquitoes and binding of the cleaved C-terminal fragment of TEP1 to bacteria in a thioester-dependent manner (Levashina et al., 2001). At present, it is unclear whether the same proteolytic activation is required for binding of TEP1 to ookinetes or whether the same C-terminal cleavage product is observed on the surface of the parasites. We are currently developing monoclonal antibodies against the N-terminal fragment of TEP1, aiming to use double staining with antibodies against the N- and C-terminal domains to answer this question.

Intriguingly, our data indicate that S and R strains exhibit an allelic polymorphism for *TEP1*: *TEP1r* is associated with the refractory L3-5 strain, whereas *TEP1s* is detected only in the susceptible G3 strain. The absence of *TEP1r* in the G3 strain, from which the L3-5 strain was selected, suggests that this allele might have been lost during breeding in our mosquito colony. It would be of interest to examine existent G3 colonies for preservation of the *TEP1r* allele in other laboratories. The comparative sequence analysis of the two alleles reveals that most of the substitutions are clustered in the C3d-like region, which contains the thioester site and, in complement factors, directly binds to substrates. In the

structural model of this region, the three loops enriched in modifications are all located on the convex surface and in close proximity to the thioester active site. The striking accumulation of polymorphisms in the thioester region might indicate its importance for the protein function. In this case, polymorphisms between *TEP1r* and *TEP1s* might affect either the reactivity of the thioester bond and/or the kinetics of protein binding to the substrate, and might account, at least partially, for the more efficient TEP1 binding and parasite killing in R mosquitoes. However, an important note of caution is that this cannot be directly demonstrated by analysis of F1 crosses. Indeed melanotic refractoriness is a complex genetic trait that has long been known to be controlled by several different genes (Zheng et al., 1997). Furthermore, it recently became clear that the complexity is even higher than previously suspected, especially as the importance of several mapped loci is dependent on the species of parasite used for infections (Zheng et al., 2003). In addition, both parental R (L3-5) and S (G3) strains are not genetically homogeneous (Zheng et al., 2003). Although we have performed reciprocal RxS crosses and observed that the transheterozygotes (*TEP1r/TEP1s*) are intermediate between the R and S phenotypes (data not shown), this does not in itself prove that the difference of the strains results from the TEP1 polymorphisms. Transgenic studies will be necessary to test critically whether the expression of the *TEP1r* allele in the genetic background of S mosquitoes is sufficient to accelerate the kinetics of TEP1 binding to parasites and to augment parasite killing.

The laboratory model of infection that we have used, *A. gambiae* and *P. berghei*, is not encountered in the field. Future studies will focus in part on the role of TEP1 in the immune response of *A. gambiae* to its natural parasites. Our preliminary results indicate that TEP1 recognizes and binds to *P. falciparum* ookinetes (S.B., E.A.L. and R.E. Sinden, unpublished data), suggesting that TEP1 binding is not limited to *P. berghei*. Moreover, molecular analysis of *A. gambiae* populations points to the existence of the *TEP1s* and *TEP1r* alleles in malaria-endemic regions of West Africa (S.B., E.A.L. and D. Fontenille, unpublished data). Further studies on the genetics of natural populations will be required to examine whether the distribution of *TEP1* alleles correlates with the incidence of mosquito refractoriness in Africa.

### Experimental Procedures

#### Mosquito Colonies and Parasite Infections
The susceptible G3 and refractory L3-5 colonies were maintained as described previously (Richman et al., 1997). *P. berghei* (ANKA strain) clones 2.34 and transgenic 259cl2 (Frankle Fayard et al., submitted) were passaged in CD1 mice and parasitemia was determined from blood films stained with Diff-Quik I (Dade Behring). In most of the infection experiments, the prevalence of infection was examined 24 hpi, and was about 100%.

#### Polymorphism Detection by PCR
Genomic DNA was prepared from the parents and progeny of reciprocal crosses between susceptible G3 and refractory L3-5 mosquitoes. Specific primers for *TEP1:* Fwd: 5′-AAAGCTGTTGCGTCA-3′ Rev: 5′-ATAGTTCATTCCGTTTTGGATTACCA-3′ and for *TEP16:* Fwd as for *TEP1* Rev: 5′-CCTCTGCGTGCTTTGCTT-3′ were used at 0.3 μM to amplify fragments of 372 and 349 bp, respectively, with a standard program (30 s at 94°C; 30 s at 52°C; 45 s at 72°C) for 40 cycles.

#### Transcription Profiling by Real-Time PCR
At selected time points after infection, total RNA from at least 15 fed females was extracted with TRIzol reagent (Invitrogen) and reverse transcribed. Specific TaqMan primers and probes were designed using the Primer Express software (Applied Biosystems). *TEP1:* Fwd: 5′-AAAGCTGTTGCGTCA-3′ Rev: 5′-TTCTCCCACACACCAAACGAA-3′ and Probe: 5′-FAM-CCAGATGCGTTACCGCCAGACAGATG-TAMRA-3′; *TEP16:* Fwd as for *TEP1*, Rev 5′-ATTAGTAGTCTCCCACAAACCAAAT-3′ and Probe 5′-FAM-CCAGATGCGCTACCGTCAGACGGATG-TAMRA-3′; *S7:* Fwd 5′-AGCAGCTACAGCACTTGATTATTGG-3′, Rev 5′-GATATTTTTAACGGCTTTTCTGCGT-3′ and Probe 5′-FAM-CCCGATTTCTCCGATCTTTCACATTCCA-TAMRA-3′. The PCR reactions were assembled and run in the ABI PRIS 7000 Sequence Detection System (Applied Biosystems) following the manufacturer's instructions.

#### Immunostainings for Confocal and Electron Microscopy
Immunostainings were performed essentially as described (Danielli et al., 2000). For confocal analysis, after blocking, midguts and abdomen walls were incubated overnight at 4°C with a mixture of primary antibodies (rabbit polyclonal antibody against TEP1 at 1:350, mouse monoclonal antibody against *P. berghei* P28 (gift from R. Sinden) at 1:1000, mouse polyclonal antibody against *P. berghei* TRAP (gift from S. Naitza and A. Chrisanti) at 1:300, rat polyclonal antibody against PPO6 (gift from H.-M. Mueller) at 1:500) followed by 1 hr incubation with secondary antibodies (The Jackson Laboratory, 1:2000). Cell nuclei were colored with DAPI (Roche Applied Science, 1 ng/mL). Samples were mounted using the ProLong Antifade Kit (Molecular Probes) and analyzed under a Zeiss LSM 510 confocal microscope. For electron microscopy analysis, midguts were dissected 30 hr postinfection and fixed in 1% paraformaldehyde, 0.5% glutaraldehyde in 0.1 M phosphate buffer [pH 7.2] for 1 hr. After permeabilization and blocking, midguts were incubated overnight at 4°C with rabbit polyclonal antibody against TEP1 at 1:100, followed by 1 hr incubation with a 10 nm gold particle-conjugated secondary antibody (British BioCell International, 1:60). The samples were then dehydrated, embedded in epoxy resin and sectioned for examination with an electron microscope (BioTwin, Phillips).

#### Double-Stranded RNA Knockdown
dsRNAs were produced as described previously using the plasmids pLL6ds for *dsGFP*, pLL17 for *dsTEP1* (Levashina et al., 2001), and pLL100 for *dsLacZ*. The 816 bp ClaI-BamHI fragment of pC4 (Thummel and Pirrotta, 1991) was cloned between the two T7 promoters of pLL10, resulting in pLL100. Adult females were injected with dsRNA (3 mg/mL) and allowed to recover for 4 days before infection (Blandin et al., 2002) or before collecting hemolymph for immunoblotting (Levashina et al., 2001). The specificity of the knockdown was examined using TEP1-specific antibodies as well as rabbit polyclonal antibodies against other members of TEP family (TEP2, 3 and 4).

#### Infection Intensity and Mean Oocyst Numbers in Mosquitoes
For each experiment, mosquitoes were blood-fed on a parasite-infected mouse. Mosquito midguts were dissected 6–11 days later and numbers of oocysts were counted using a Zeiss fluorescence microscope.

**References**

Alavi, Y., Arai, M., Mendoza, J., Tufet-Bayona, M., Sinha, R., Fowler, K., Billker, O., Franke-Fayard, B., Janse, C.J., Waters, A., and Sinden, R.E. (2003). The dynamics of interactions between *Plasmodium* and the mosquito: a study of the infectivity of *Plasmodium berghei* and *Plasmodium gallinaceum*, and their transmission by *Anopheles stephensi*, *Anopheles gambiae* and *Aedes aegypti*. Int. J. Parasitol. *33*, 933–943.

Blandin, S., Moita, L.F., Köcher, T., Wilm, M., Kafatos, F.C., and Levashina, E.A. (2002). Reverse genetics in the mosquito *Anopheles gambiae*: targeted disruption of the *Defensin* gene. EMBO Rep. *3*, 852–856.

Carroll, M.C., and Fischer, M.B. (1997). Complement and the immune response. Curr. Opin. Immunol. *9*, 64–69.

Christophides, G.K., Zdobnov, E., Barillas-Mury, C., Birney, E., Blandin, S., Blass, C., Brey, P.T., Collins, F.H., Danielli, A., Dimopoulos, G., et al. (2002). Immunity-related genes and gene families in *Anopheles gambiae*. Science *298*, 159–165.

Collins, F.H., Sakai, R.K., Vernick, K.D., Paskewitz, S., Seeley, D.C., Miller, L.H., Collins, W.E., Campbell, C.C., and Gwadz, R.W. (1986). Genetic selection of a *Plasmodium*-refractory strain of the malaria vector *Anopheles gambiae*. Science *234*, 607–610.

Danielli, A., Loukeris, T.G., Lagueux, M., Müller, H.M., Richman, A., and Kafatos, F.C. (2000). A modular chitin-binding protease associated with hemocytes and hemolymph in the mosquito *Anopheles gambiae*. Proc. Natl. Acad. Sci. USA *97*, 7136–7141.

Dimopoulos, G., Christophides, G.K., Meister, S., Schultz, J., White, K.P., Barillas-Mury, C., and Kafatos, F.C. (2002). Genome expression analysis of *Anopheles gambiae*: responses to injury, bacterial challenge, and malaria infection. Proc. Natl. Acad. Sci. USA *99*, 8814–8819.

Law, S.K., and Dodds, A.W. (1997). The internal thioester and the covalent binding properties of the complement proteins C3 and C4. Protein Sci. *6*, 263–274.

Levashina, E.A., Moita, L.F., Blandin, S., Vriend, G., Lagueux, M., and Kafatos, F.C. (2001). Conserved role of a complement-like protein in phagocytosis revealed by dsRNA knockout in cultured cells of the mosquito, *Anopheles gambiae*. Cell *104*, 709–718.

Meis, J.F., Pool, G., van Gemert, G.J., Lensen, A.H., Ponnudurai, T., and Meuwissen, J.H. (1989). *Plasmodium falciparum* ookinetes migrate intercellularly through *Anopheles stephensi* midgut epithelium. Parasitol. Res. *76*, 13–19.

Müller, H.M., Dimopoulos, G., Blass, C., and Kafatos, F.C. (1999). A hemocyte-like cell line established from the malaria vector *Anopheles gambiae* expresses six prophenoloxidase genes. J. Biol. Chem. *274*, 11727–11735.

Richman, A.M., Dimopoulos, G., Seeley, D., and Kafatos, F.C. (1997). *Plasmodium* activates the innate immune response of *Anopheles gambiae* mosquitoes. EMBO J. *16*, 6114–6119.

Simonetti, A.B., Billingsley, P.F., Winger, L.A., and Sinden, R.E. (1993). Kinetics of expression of two major *Plasmodium berghei* antigens in the mosquito vector, *Anopheles stephensi*. J. Eukaryot. Microbiol. *40*, 569–576.

Snow, R.W., Craig, M., Deichmann, U., and Marsh, K. (1999). Estimating mortality, morbidity and disability due to malaria among Africa's non-pregnant population. Bull. World Health Organ. *77*, 624–640.

Thummel, C.S., and Pirrotta, V. (1991). Technical notes: New pCasPer P-element vectors. Dros. Info. Service *71*, 150.

Vargas, L. (1949). Culicine and aedine mosquitoes and the malaria infections of lower animals. In Malariology, M.F. Boyd, ed. (Philadelphia: W.B. Saunders Company), pp. 526–538.

Vernick, K.D., Fujioka, H., Seeley, D.C., Tandler, B., Aikawa, M., and Miller, L.H. (1995). *Plasmodium gallinaceum*: a refractory mechanism of ookinete killing in the mosquito, *Anopheles gambiae*. Exp. Parasitol. *80*, 583–595.

Zheng, L., Cornel, A.J., Wang, R., Erfle, H., Voss, H., Ansorge, W., Kafatos, F.C., and Collins, F.H. (1997). Quantitative trait loci for refractoriness of *Anopheles gambiae* to *Plasmodium cynomolgi* B. Science *276*, 425–428.

Zheng, L., Wang, S., Romans, P., Zhao, H., Luna, C., and Benedict, M.Q. (2003). Quantitative trait loci in *Anopheles gambiae* controlling the encapsulation response against *Plasmodium cynomolgi* Ceylon. BMC Genet. *4*, 16.